Search for W' bosons decaying to an electron and a neutrino with the D0 detector

V.M. Abazov[36], B. Abbott[76], M. Abolins[66], B.S. Acharya[29], M. Adams[52], T. Adams[50], E. Aguilo[6], S.H. Ahn[31], M. Ahsan[60], G.D. Alexeev[36], G. Alkhazov[40], A. Alton[65,a], G. Alverson[64], G.A. Alves[2], M. Anastasoaie[35], L.S. Ancu[35], T. Andeen[54], S. Anderson[46], B. Andrieu[17], M.S. Anzelc[54], Y. Arnoud[14], M. Arov[61], M. Arthaud[18], A. Askew[50], B. Åsman[41], A.C.S. Assis Jesus[3], O. Atramentov[50], C. Autermann[21], C. Avila[8], C. Ay[24], F. Badaud[13], A. Baden[62], L. Bagby[53], B. Baldin[51], D.V. Bandurin[60], S. Banerjee[29], P. Banerjee[29], E. Barberis[64], A.-F. Barfuss[15], P. Bargassa[81], P. Baringer[59], J. Barreto[2], J.F. Bartlett[51], U. Bassler[18], D. Bauer[44], S. Beale[6], A. Bean[59], M. Begalli[3], M. Begel[72], C. Belanger-Champagne[41], L. Bellantoni[51], A. Bellavance[51], J.A. Benitez[66], S.B. Beri[27], G. Bernardi[17], R. Bernhard[23], I. Bertram[43], M. Besançon[18], R. Beuselinck[44], V.A. Bezzubov[39], P.C. Bhat[51], V. Bhatnagar[27], C. Biscarat[20], G. Blazey[53], F. Blekman[44], S. Blessing[50], D. Bloch[19], K. Bloom[68], A. Boehnlein[51], D. Boline[63], T.A. Bolton[60], G. Borissov[43], T. Bose[78], A. Brandt[79], R. Brock[66], G. Brooijmans[71], A. Bross[51], D. Brown[82], N.J. Buchanan[50], D. Buchholz[54], M. Buehler[82], V. Buescher[22], S. Bunichev[38], S. Burdin[43,b], S. Burke[46], T.H. Burnett[83], C.P. Buszello[44], J.M. Butler[63], P. Calfayan[25], S. Calvet[16], J. Cammin[72], W. Carvalho[3], B.C.K. Casey[51], N.M. Cason[56], H. Castilla-Valdez[33], S. Chakrabarti[18], D. Chakraborty[53], K.M. Chan[56], K. Chan[6], A. Chandra[49], F. Charles[19,‡], E. Cheu[46], F. Chevallier[14], D.K. Cho[63], S. Choi[32], B. Choudhary[28], L. Christofek[78], T. Christoudias[44,†], S. Cihangir[51], D. Claes[68], Y. Coadou[6], M. Cooke[81], W.E. Cooper[51], M. Corcoran[81], F. Couderc[18], M.-C. Cousinou[15], S. Crépé-Renaudin[14], D. Cutts[78], M. Ćwiok[30], H. da Motta[2], A. Das[46], G. Davies[44], K. De[79], S.J. de Jong[35], E. De La Cruz-Burelo[65], C. De Oliveira Martins[3], J.D. Degenhardt[65], F. Déliot[18], M. Demarteau[51], R. Demina[72], D. Denisov[51], S.P. Denisov[39], S. Desai[51], H.T. Diehl[51], M. Diesburg[51], A. Dominguez[68], H. Dong[73], L.V. Dudko[38], L. Duflot[16], S.R. Dugad[29], D. Duggan[50], A. Duperrin[15], J. Dyer[66], A. Dyshkant[53], M. Eads[68], D. Edmunds[66], J. Ellison[49], V.D. Elvira[51], Y. Enari[78], S. Eno[62], P. Ermolov[38], H. Evans[55], A. Evdokimov[74], V.N. Evdokimov[39], A.V. Ferapontov[60], T. Ferbel[72], F. Fiedler[24], F. Filthaut[35], W. Fisher[51], H.E. Fisk[51], M. Ford[45], M. Fortner[53], H. Fox[23], S. Fu[51], S. Fuess[51], T. Gadfort[83], C.F. Galea[35], E. Gallas[51], E. Galyaev[56], C. Garcia[72], A. Garcia-Bellido[83], V. Gavrilov[37], P. Gay[13], W. Geist[19], D. Gelé[19], C.E. Gerber[52], Y. Gershtein[50], D. Gillberg[6], G. Ginther[72], N. Gollub[41], B. Gómez[8], A. Goussiou[56], P.D. Grannis[73], H. Greenlee[51], Z.D. Greenwood[61], E.M. Gregores[4], G. Grenier[20], Ph. Gris[13], J.-F. Grivaz[16], A. Grohsjean[25], S. Grünendahl[51], M.W. Grünewald[30], J. Guo[73], F. Guo[73], P. Gutierrez[76], G. Gutierrez[51], A. Haas[71], N.J. Hadley[62], P. Haefner[25], S. Hagopian[50], J. Haley[69], I. Hall[66], R.E. Hall[48], L. Han[7], K. Hanagaki[51], P. Hansson[41], K. Harder[45], A. Harel[72], R. Harrington[64], J.M. Hauptman[58], R. Hauser[66], J. Hays[44], T. Hebbeker[21], D. Hedin[53], J.G. Hegeman[34], J.M. Heinmiller[52], A.P. Heinson[49], U. Heintz[63], C. Hensel[59], K. Herner[73], G. Hesketh[64], M.D. Hildreth[56], R. Hirosky[82], J.D. Hobbs[73], B. Hoeneisen[12], H. Hoeth[26], M. Hohlfeld[22], S.J. Hong[31], S. Hossain[76], P. Houben[34], Y. Hu[73], Z. Hubacek[10], V. Hynek[9], I. Iashvili[70], R. Illingworth[51], A.S. Ito[51], S. Jabeen[63], M. Jaffré[16], S. Jain[76], K. Jakobs[23], C. Jarvis[62], R. Jesik[44], K. Johns[46], C. Johnson[71], M. Johnson[51], A. Jonckheere[51], P. Jonsson[44], A. Juste[51], D. Käfer[21], E. Kajfasz[15], A.M. Kalinin[36], J.R. Kalk[66], J.M. Kalk[61], S. Kappler[21], D. Karmanov[38], P. Kasper[51], I. Katsanos[71], D. Kau[50], R. Kaur[27], V. Kaushik[79], R. Kehoe[80], S. Kermiche[15], N. Khalatyan[51], A. Khanov[77], A. Kharchilava[70], Y.M. Kharzheev[36], D. Khatidze[71], H. Kim[32], T.J. Kim[31], M.H. Kirby[54], M. Kirsch[21], B. Klima[51], J.M. Kohli[27], J.-P. Konrath[23], M. Kopal[76], V.M. Korablev[39], A.V. Kozelov[39], D. Krop[55], T. Kuhl[24], A. Kumar[70], S. Kunori[62], A. Kupco[11], T. Kurča[20], J. Kvita[9], F. Lacroix[13], D. Lam[56], S. Lammers[71], G. Landsberg[78], P. Lebrun[20], W.M. Lee[51], A. Leflat[38], F. Lehner[42], J. Lellouch[17], J. Leveque[46], P. Lewis[44], J. Li[79], Q.Z. Li[51], L. Li[49], S.M. Lietti[5], J.G.R. Lima[53], D. Lincoln[51], J. Linnemann[66], V.V. Lipaev[39], R. Lipton[51], Y. Liu[7,†], Z. Liu[6], L. Lobodenko[40], M. Lokajicek[11], P. Love[43], H.J. Lubatti[83], A.L. Lyon[51], A.K.A. Maciel[2], D. Mackin[81], R.J. Madaras[47], P. Mättig[26], C. Magass[21], A. Magerkurth[65], P.K. Mal[56], H.B. Malbouisson[3], S. Malik[68], V.L. Malyshev[36], H.S. Mao[51], Y. Maravin[60], B. Martin[14], R. McCarthy[73], A. Melnitchouk[67], A. Mendes[15], L. Mendoza[8], P.G. Mercadante[5], M. Merkin[38], K.W. Merritt[51], J. Meyer[22,d], A. Meyer[21], T. Millet[20], J. Mitrevski[71], J. Molina[3], R.K. Mommsen[45], N.K. Mondal[29], R.W. Moore[6], T. Moulik[59], G.S. Muanza[20], M. Mulders[51], M. Mulhearn[71], O. Mundal[22], L. Mundim[3], E. Nagy[15], M. Naimuddin[51], M. Narain[78], N.A. Naumann[35], H.A. Neal[65], J.P. Negret[8], P. Neustroev[40], H. Nilsen[23], H. Nogima[3], A. Nomerotski[51], S.F. Novaes[5], T. Nunnemann[25], V. O'Dell[51], D.C. O'Neil[6], G. Obrant[40], C. Ochando[16], D. Onoprienko[60], N. Oshima[51], J. Osta[56], R. Otec[10], G.J. Otero y Garzón[51], M. Owen[45], P. Padley[81], M. Pangilinan[78], N. Parashar[57],

S.-J. Park[72], S.K. Park[31], J. Parsons[71], R. Partridge[78], N. Parua[55], A. Patwa[74], G. Pawloski[81], B. Penning[23], M. Perfilov[38], K. Peters[45], Y. Peters[26], P. Pétroff[16], M. Petteni[44], R. Piegaia[1], J. Piper[66], M.-A. Pleier[22], P.L.M. Podesta-Lerma[33,c], V.M. Podstavkov[51], Y. Pogorelov[56], M.-E. Pol[2], P. Polozov[37], B.G. Pope[66], A.V. Popov[39], C. Potter[6], W.L. Prado da Silva[3], H.B. Prosper[50], S. Protopopescu[74], J. Qian[65], A. Quadt[22,d], B. Quinn[67], A. Rakitine[43], M.S. Rangel[2], K. Ranjan[28], P.N. Ratoff[43], P. Renkel[80], S. Reucroft[64], P. Rich[45], M. Rijssenbeek[73], I. Ripp-Baudot[19], F. Rizatdinova[77], S. Robinson[44], R.F. Rodrigues[3], M. Rominsky[76], C. Royon[18], P. Rubinov[51], R. Ruchti[56], G. Safronov[37], G. Sajot[14], A. Sánchez-Hernández[33], M.P. Sanders[17], A. Santoro[3], G. Savage[51], L. Sawyer[61], T. Scanlon[44], D. Schaile[25], R.D. Schamberger[73], Y. Scheglov[40], H. Schellman[54], P. Schieferdecker[25], T. Schliephake[26], C. Schwanenberger[45], A. Schwartzman[69], R. Schwienhorst[66], J. Sekaric[50], H. Severini[76], E. Shabalina[52], M. Shamim[60], V. Shary[18], A.A. Shchukin[39], R.K. Shivpuri[28], V. Siccardi[19], V. Simak[10], V. Sirotenko[51], P. Skubic[76], P. Slattery[72], D. Smirnov[56], J. Snow[75], G.R. Snow[68], S. Snyder[74], S. Söldner-Rembold[45], L. Sonnenschein[17], A. Sopczak[43], M. Sosebee[79], K. Soustruznik[9], M. Souza[2], B. Spurlock[79], J. Stark[14], J. Steele[61], V. Stolin[37], D.A. Stoyanova[39], J. Strandberg[65], S. Strandberg[41], M.A. Strang[70], M. Strauss[76], E. Strauss[73], R. Ströhmer[25], D. Strom[54], L. Stutte[51], S. Sumowidagdo[50], P. Svoisky[56], A. Sznajder[3], M. Talby[15], P. Tamburello[46], A. Tanasijczuk[1], W. Taylor[6], J. Temple[46], B. Tiller[25], F. Tissandier[13], M. Titov[18], V.V. Tokmenin[36], T. Toole[62], I. Torchiani[23], T. Trefzger[24], D. Tsybychev[73], B. Tuchming[18], C. Tully[69], P.M. Tuts[71], R. Unalan[66], S. Uvarov[40], L. Uvarov[40], S. Uzunyan[53], B. Vachon[6], P.J. van den Berg[34], R. Van Kooten[55], W.M. van Leeuwen[34], N. Varelas[52], E.W. Varnes[46], I.A. Vasilyev[39], M. Vaupel[26], P. Verdier[20], L.S. Vertogradov[36], M. Verzocchi[51], F. Villeneuve-Seguier[44], P. Vint[44], P. Vokac[10], E. Von Toerne[60], M. Voutilainen[68,e], R. Wagner[69], H.D. Wahl[50], L. Wang[62], M.H.L.S Wang[51], J. Warchol[56], G. Watts[83], M. Wayne[56], M. Weber[51], G. Weber[24], A. Wenger[23,f], N. Wermes[22], M. Wetstein[62], A. White[79], D. Wicke[26], G.W. Wilson[59], S.J. Wimpenny[49], M. Wobisch[61], D.R. Wood[64], T.R. Wyatt[45], Y. Xie[78], S. Yacoob[54], R. Yamada[51], M. Yan[62], T. Yasuda[51], Y.A. Yatsunenko[36], K. Yip[74], H.D. Yoo[78], S.W. Youn[54], J. Yu[79], A. Zatserklyaniy[53], C. Zeitnitz[26], T. Zhao[83], B. Zhou[65], J. Zhu[73], M. Zielinski[72], D. Zieminska[55], A. Zieminski[55], L. Zivkovic[71], V. Zutshi[53], and E.G. Zverev[38]

(The DØ Collaboration)

[1] Universidad de Buenos Aires, Buenos Aires, Argentina
[2] LAFEX, Centro Brasileiro de Pesquisas Físicas, Rio de Janeiro, Brazil
[3] Universidade do Estado do Rio de Janeiro, Rio de Janeiro, Brazil
[4] Universidade Federal do ABC, Santo André, Brazil
[5] Instituto de Física Teórica, Universidade Estadual Paulista, São Paulo, Brazil
[6] University of Alberta, Edmonton, Alberta, Canada, Simon Fraser University, Burnaby, British Columbia, Canada, York University, Toronto, Ontario, Canada, and McGill University, Montreal, Quebec, Canada
[7] University of Science and Technology of China, Hefei, People's Republic of China
[8] Universidad de los Andes, Bogotá, Colombia
[9] Center for Particle Physics, Charles University, Prague, Czech Republic
[10] Czech Technical University, Prague, Czech Republic
[11] Center for Particle Physics, Institute of Physics, Academy of Sciences of the Czech Republic, Prague, Czech Republic
[12] Universidad San Francisco de Quito, Quito, Ecuador
[13] Laboratoire de Physique Corpusculaire, IN2P3-CNRS, Université Blaise Pascal, Clermont-Ferrand, France
[14] Laboratoire de Physique Subatomique et de Cosmologie, IN2P3-CNRS, Universite de Grenoble 1, Grenoble, France
[15] CPPM, IN2P3-CNRS, Université de la Méditerranée, Marseille, France
[16] Laboratoire de l'Accélérateur Linéaire, IN2P3-CNRS et Université Paris-Sud, Orsay, France
[17] LPNHE, IN2P3-CNRS, Universités Paris VI and VII, Paris, France
[18] DAPNIA/Service de Physique des Particules, CEA, Saclay, France
[19] IPHC, Université Louis Pasteur et Université de Haute Alsace, CNRS, IN2P3, Strasbourg, France
[20] IPNL, Université Lyon 1, CNRS/IN2P3, Villeurbanne, France and Université de Lyon, Lyon, France
[21] III. Physikalisches Institut A, RWTH Aachen, Aachen, Germany
[22] Physikalisches Institut, Universität Bonn, Bonn, Germany
[23] Physikalisches Institut, Universität Freiburg, Freiburg, Germany
[24] Institut für Physik, Universität Mainz, Mainz, Germany
[25] Ludwig-Maximilians-Universität München, München, Germany
[26] Fachbereich Physik, University of Wuppertal, Wuppertal, Germany

[27] *Panjab University, Chandigarh, India*
[28] *Delhi University, Delhi, India*
[29] *Tata Institute of Fundamental Research, Mumbai, India*
[30] *University College Dublin, Dublin, Ireland*
[31] *Korea Detector Laboratory, Korea University, Seoul, Korea*
[32] *SungKyunKwan University, Suwon, Korea*
[33] *CINVESTAV, Mexico City, Mexico*
[34] *FOM-Institute NIKHEF and University of Amsterdam/NIKHEF, Amsterdam, The Netherlands*
[35] *Radboud University Nijmegen/NIKHEF, Nijmegen, The Netherlands*
[36] *Joint Institute for Nuclear Research, Dubna, Russia*
[37] *Institute for Theoretical and Experimental Physics, Moscow, Russia*
[38] *Moscow State University, Moscow, Russia*
[39] *Institute for High Energy Physics, Protvino, Russia*
[40] *Petersburg Nuclear Physics Institute, St. Petersburg, Russia*
[41] *Lund University, Lund, Sweden, Royal Institute of Technology and Stockholm University,
Stockholm, Sweden, and Uppsala University, Uppsala, Sweden*
[42] *Physik Institut der Universität Zürich, Zürich, Switzerland*
[43] *Lancaster University, Lancaster, United Kingdom*
[44] *Imperial College, London, United Kingdom*
[45] *University of Manchester, Manchester, United Kingdom*
[46] *University of Arizona, Tucson, Arizona 85721, USA*
[47] *Lawrence Berkeley National Laboratory and University of California, Berkeley, California 94720, USA*
[48] *California State University, Fresno, California 93740, USA*
[49] *University of California, Riverside, California 92521, USA*
[50] *Florida State University, Tallahassee, Florida 32306, USA*
[51] *Fermi National Accelerator Laboratory, Batavia, Illinois 60510, USA*
[52] *University of Illinois at Chicago, Chicago, Illinois 60607, USA*
[53] *Northern Illinois University, DeKalb, Illinois 60115, USA*
[54] *Northwestern University, Evanston, Illinois 60208, USA*
[55] *Indiana University, Bloomington, Indiana 47405, USA*
[56] *University of Notre Dame, Notre Dame, Indiana 46556, USA*
[57] *Purdue University Calumet, Hammond, Indiana 46323, USA*
[58] *Iowa State University, Ames, Iowa 50011, USA*
[59] *University of Kansas, Lawrence, Kansas 66045, USA*
[60] *Kansas State University, Manhattan, Kansas 66506, USA*
[61] *Louisiana Tech University, Ruston, Louisiana 71272, USA*
[62] *University of Maryland, College Park, Maryland 20742, USA*
[63] *Boston University, Boston, Massachusetts 02215, USA*
[64] *Northeastern University, Boston, Massachusetts 02115, USA*
[65] *University of Michigan, Ann Arbor, Michigan 48109, USA*
[66] *Michigan State University, East Lansing, Michigan 48824, USA*
[67] *University of Mississippi, University, Mississippi 38677, USA*
[68] *University of Nebraska, Lincoln, Nebraska 68588, USA*
[69] *Princeton University, Princeton, New Jersey 08544, USA*
[70] *State University of New York, Buffalo, New York 14260, USA*
[71] *Columbia University, New York, New York 10027, USA*
[72] *University of Rochester, Rochester, New York 14627, USA*
[73] *State University of New York, Stony Brook, New York 11794, USA*
[74] *Brookhaven National Laboratory, Upton, New York 11973, USA*
[75] *Langston University, Langston, Oklahoma 73050, USA*
[76] *University of Oklahoma, Norman, Oklahoma 73019, USA*
[77] *Oklahoma State University, Stillwater, Oklahoma 74078, USA*
[78] *Brown University, Providence, Rhode Island 02912, USA*
[79] *University of Texas, Arlington, Texas 76019, USA*
[80] *Southern Methodist University, Dallas, Texas 75275, USA*
[81] *Rice University, Houston, Texas 77005, USA*
[82] *University of Virginia, Charlottesville, Virginia 22901, USA and*
[83] *University of Washington, Seattle, Washington 98195, USA*

(Dated: November 23, 2007)

This Letter describes the search for a new heavy charged gauge boson W' decaying into an electron and a neutrino. The data were collected with the D0 detector at the Fermilab Tevatron $p\bar{p}$ Collider at $\sqrt{s} = 1.96$ TeV, and correspond to an integrated luminosity of about 1 fb^{-1}. Lacking any significant excess in the data in comparison with known processes, an upper limit is set on $\sigma_{W'} \times B(W' \to e\nu)$,

and a W' boson with mass below 1.00 TeV can be excluded at the 95% C.L., assuming standard-model-like couplings to fermions. This result significantly improves upon previous limits, and is the most stringent to date.

PACS numbers: 12.60.Cn, 13.85.Rm, 14.70.Pw

The standard model (SM) describes the fundamental fermions and their interactions via gauge bosons at a high level of accuracy, but it is not considered to be a complete theory. Additional gauge bosons are introduced in *e. g.* left-right-symmetric models (broken $SU(2)_L \times SU(2)_R$) or in grand unified theories which may also involve supersymmetry (*e. g.* E_6) [1]. Assuming the most general case, a new gauge group can comprise a new mixing angle ξ, new couplings to the fermions $\tilde{g}$ and a new CKM matrix U'. In some models the W' boson (W'^{+} or W'^{-}) is right-handed, and decays therefore into a right-handed neutrino and a charged lepton. However, such a neutrino has not yet been observed.

In this Letter we make the assumption that there is no mixing, $\tilde{g}$ is equal to the SM coupling, U' is equal to the SM CKM matrix, and that the decay channel $W' \rightarrow WZ$ is suppressed. Furthermore, the width $\Gamma_{W'}$ of the W' boson is assumed to scale with its mass $m_{W'}$,

$$\Gamma_{W'} = \frac{4}{3} \cdot \frac{m_{W'}}{m_W} \cdot \Gamma_W. \tag{1}$$

The factor of 4/3 is applied in order to account for the decay into the third quark family (*e. g.* $W' \rightarrow t\bar{b}$) which is possible for $m_{W'}$ above the kinematic threshold for this process. In case of the existence of additional generations of fermions, it is assumed that they are too heavy to be produced by a W' decay. This generic model has been introduced by Altarelli et al. [2]. It corresponds to the manifest left-right symmetric model [3] with light right-handed neutrinos if the W' boson is right-handed. In this report, the general approach [2] is considered, where the additional gauge boson W' can be right- or left-handed.

The W' boson has been searched for previously by the D0 [4–6] and the CDF experiments [7–9] in various final states. The most restrictive limit so far is $m_{W'} > 800$ GeV at the 95% C.L. [5] reported by D0 ($W' \rightarrow q\bar{q}'$, Run I).

Data collected with the D0 detector [10] at the Fermilab Tevatron $p\bar{p}$ Collider at a center-of-mass energy of 1.96 TeV are analyzed for the production of W' bosons and the subsequent decay into an electron and a neutrino. The neutrino can not be detected, but it gives rise to missing transverse energy ($\not{E}_T$) in the detector. The dataset corresponds to an integrated luminosity [11] of 0.99 ± 0.06 fb^{-1}, and was collected between 2002 and 2006 during Run II of the Tevatron.

The D0 detector has a central-tracking system, consisting of a silicon microstrip tracker (SMT) and a central fiber tracker (CFT), both located within a 2 T superconducting solenoidal magnet, with designs optimized for tracking and vertexing at $|\eta| < 3$ and $|\eta| < 2.5$, respectively, where $\eta = -\ln \tan \frac{\theta}{2}$ is the pseudorapidity and θ the polar angle with respect to the z-axis (proton-beam direction). A liquid-argon and uranium calorimeter has a central section (CC) covering pseudorapidities $|\eta|$ up to ≈ 1.1, and two end calorimeters (EC) that extend coverage to $|\eta| \approx 4.2$, each housed in separate cryostats. An outer muon system, at $|\eta| < 2$, consists of a layer of tracking detectors and scintillation trigger counters in front of 1.8 T iron toroids, followed by two similar layers after the toroids. Luminosity is measured using plastic scintillator arrays placed in front of the EC cryostats.

Different SM processes contribute to the electron and $\not{E}_T$ final state: inclusive production of W or Z bosons, di-bosons (WW, WZ, ZZ) or $t\bar{t}$ pairs in which at least one boson or one top quark decays into electrons directly or via tau decays. In these processes the missing energy is due to the neutrino. There are also two sources of misidentification background that can contribute to the electron and $\not{E}_T$ final state: QCD multijet background with one jet misidentified as an electron and energy mismeasurement which can cause large $\not{E}_T$ either along or in the opposite direction of the electron, and $Z \rightarrow ee$ events where one electron is lost (*e. g.* entering non-instrumented sections of the calorimeter) or misreconstructed. The latter case can lead to large $\not{E}_T$.

The W' signal and SM processes (including $Z \rightarrow ee$) have been simulated with the PYTHIA 6.323 [12] Monte Carlo program using the CTEQ6L1 [13] parton distribution functions (PDFs), except for the QCD multijet background, which is estimated from data. The generated events are passed through a detailed detector simulation based on GEANT [14], and combined with randomly triggered events from data to simulate the effects of pileup. Higher order corrections to the PYTHIA leading order cross sections (K factors) have been applied. The next-to-next-to-leading order (NNLO) K factors and errors due to PDF uncertainties for the signal, the W and the Z samples are extracted from Ref. [15]; the NNLO (NLO) cross section for $t\bar{t}$ (di-boson) production is taken from Ref. [16] ([17]).

The signal cross section falls steeply with increasing mass of the W' boson. In addition, for very large masses the on-mass-shell production of W' bosons is heavily suppressed due to the smallness of the PDFs at large x. As shown in Fig. 1, the transverse mass distribution no longer exhibits a pronounced peak. The transverse mass m_T is calculated from the transverse energy of the electron, $E_T^{\rm el}$, the missing transverse energy, $\not{E}_T$, and the azimuth angle [18] difference between the electron and
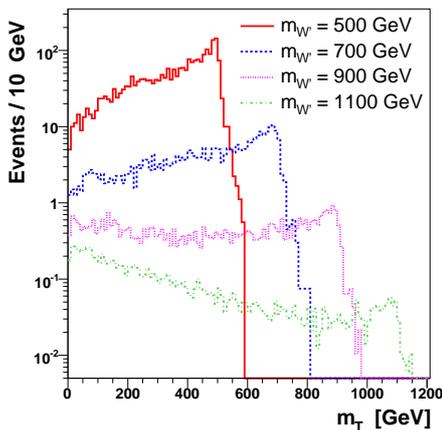
FIG. 1: Transverse mass m_T distributions for different masses of the W' boson (generator level, PYTHIA). The event numbers correspond to an integrated luminosity of 1 fb^{-1}.

$\not{E}_T$ via

$$m_T = \sqrt{2E_T^{\mathrm{el}}\not{E}_T(1 - \cos\Delta\phi(\text{electron}, \not{E}_T))}. \quad (2)$$

Events triggered by a set of inclusive single electron triggers are considered. Electrons with $E_T^{\mathrm{el}} > 30$ GeV passing the offline identification criteria are selected. Monte Carlo studies have shown that the majority ($\approx$ 80%) of the electrons stemming from the W' decays are emitted into the central detector region. Since the forward detector region exhibits a small signal-to-background ratio, only electrons reconstructed in the CC are used in the analysis. Electromagnetic clusters are built around a calorimeter seed. Such clusters consist of cells in a cone ($\Delta R = \sqrt{(\Delta\eta)^2 + (\Delta\phi)^2} < 0.4$) around the seed. Furthermore, the electron shower is required to be isolated in the calorimeter, and to deposit most of its energy ($> 90\%$) in the electromagnetic part of the calorimeter. The isolation $I = [E_{\mathrm{tot}}^{0.4} - E_{\mathrm{EM}}^{0.2}]/E_{\mathrm{EM}}^{0.2}$, which uses the total shower energy, $E_{\mathrm{tot}}^{0.4}$, in a cone of radius $R = 0.4$ and the electromagnetic energy, $E_{\mathrm{EM}}^{0.2}$, in a cone of radius $R = 0.2$, is required to be less than 0.2. A cut on the electron shower shape variable is applied to separate electromagnetic from hadronic showers. The electron is required to have a track matched in z and ϕ direction and to stem from the primary vertex. Correction factors are applied to the simulated events in order to take differences in the reconstruction efficiencies observed in data and Monte Carlo into account. Finally, the energy dependence of the basic electron reconstruction criteria has been studied with simulated electrons from W' decays. The reconstruction efficiency is found to be constant (94 ± 1 %) and does not exhibit a visible energy dependence within the statistical uncertainties of the Monte Carlo samples. The $\not{E}_T$ is calculated from all calorimeter cells. Corrections are applied to account for the electromagnetic and jet energy scales. We require

$\not{E}_T > 30$ GeV.

Since the transverse momentum of the neutrino is expected to be balanced by the electron transverse energy in signal events, a selection on the ratio of the energies is applied, $0.6 < E_T^{\mathrm{el}}/\not{E}_T < 1.4$. This requirement reduces instrumental backgrounds from misidentified $\not{E}_T$. Jets are reconstructed with the iterative mid-point cone algorithm ($R = 0.5$) [19]. If any jets with $p_T > 15$ GeV are present in the event, we require $\Delta\phi(\text{jet, electron}) < 2.8$ and $\Delta\phi(\text{jet}, \not{E}_T) < 2.8$. These selections remove events from QCD multijet production.

The contribution from QCD multijet events is estimated using a control sample derived from data with the same kinematic cuts. In this sample, the electron candidate fails the shower shape requirement. The resulting events are normalized to the data sample. The scale factor for the entire QCD multijet sample is adjusted in the low reconstructed transverse mass region ($m_T < 30$ GeV), which is dominated by QCD multijet background events, such that the sum of the PYTHIA Monte Carlo prediction and the QCD multijet sample describes the data as shown in Fig. 2(a). The data are normalized to W boson production and decay in the $e\nu$ mode using the W peak region (60 GeV $< m_T < 140$ GeV, as shown in Fig. 2(a)) because many efficiency and acceptance errors largely cancel in this ratio. We use the theoretical prediction for the W boson production cross section $\sigma_W \times B(W \to e\nu) = 2583_{-84}^{+94}$ pb from Ref. [15].

Jets may be present in conjunction with a W boson due to higher order QCD contributions. Since PYTHIA does not properly describe the transverse momentum distribution of the W boson in such processes, this spectrum is separately reweighted in events with one, two and three jets in order to match the distributions observed in the data. This correction affects 10% of the W Monte Carlo events. The sample defined by the selection cuts mentioned above contains 452,984 data events compared to $454,000 \pm 35,000$ events expected from SM processes and instrumental backgrounds after applying all corrections.

The tail of the spectrum ($m_T > 140$ GeV) is now considered to search for $W' \to e\nu$. A good agreement between the data and the background prediction can be observed as shown in Fig. 2(b, c). In the data 37 (2) events are reconstructed with $m_T > 300$ GeV (500 GeV) compared to a prediction of 37.1 ± 2.1 (stat) $_{-3.7}^{+6.0}$ (sys) (2.3 ± 0.5 (stat) $_{-0.7}^{+0.5}$ (sys)) background events. In Table I, the breakdown of the individual contributions of the various background processes is given, including expected numbers of signal events. Two kinds of systematic uncertainties contribute in this analysis (the relative uncertainties quoted below always relate to the tail of the transverse mass spectrum because only this region is used for the search). The uncertainties of the normalization in the W peak region (4%), the cross sections of the SM processes (4-10%), the electron reconstruction efficiency corrections (2%) and the scale factor for the QCD
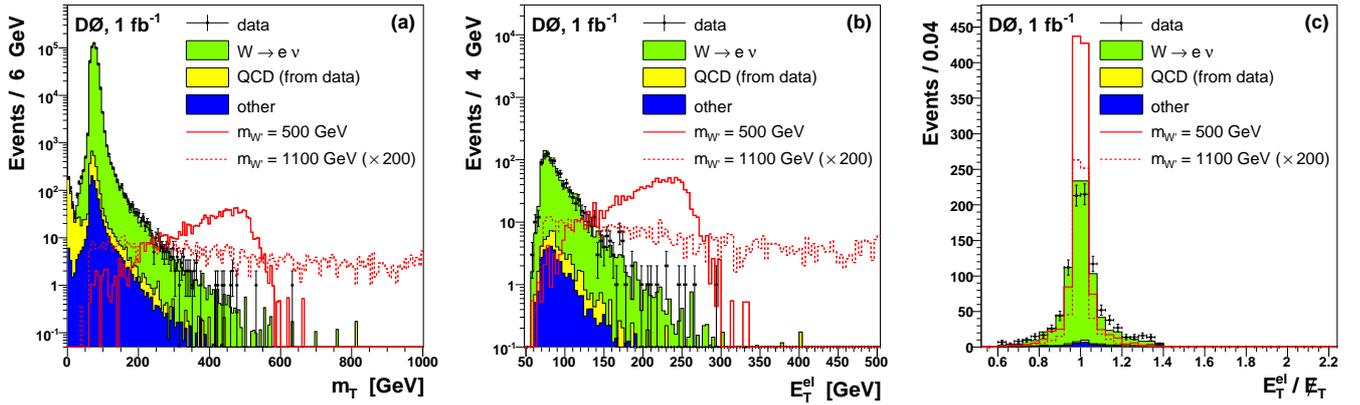
FIG. 2: Comparison between data and background prediction: (a) Distribution of the transverse mass m_T; (b) distribution of the electron transverse energy E_T^{el} in events with $m_T > 140$ GeV; (c) distribution of the ratio of electron transverse energy and $\not{E}_T$ in events with $m_T > 140$ GeV. The signal is shown for two different masses of the W' boson.

multijet sample (7%) affect only the global normalization. Uncertainties on the PDFs, electron energy scale and resolution, jet energy scale, decay width Γ_W of the W boson, and the transverse momentum of the W boson lead to changes of the shape of the distributions.

In order to study the effect of the electron energy scale and resolution, the electron energies have been varied within the known uncertainties. The variations of scale and resolution are performed independently. The $\not{E}_T$ is recalculated after varying the electron energy. The overall uncertainty on the event numbers is large for the W sample (4%), but small for the W' signal ($< 1\%$ for 500 GeV $< m_{W'} < 1200$ GeV). The uncertainty of the energy resolution is an order of magnitude smaller than the energy scale uncertainty. In order to study the PDF uncertainty, the Monte Carlo events which have been produced using CTEQ6L1 PDFs are reweighted to CTEQ6.1M.xx (xx = 0, . . . , 40), making use of the CTEQ6.1M PDFs and the 40 error functions [13]. The overall uncertainty varies between 3% ($m_{W'} = 500$ GeV) and 8% ($m_{W'} = 1200$ GeV). For the W sample an uncertainty of 3% is derived. The width of the W boson is known to about 2% [20]. This can cause a shift ($\sim 4\%$) of the tail of the transverse mass distribution of the W boson. Finally, the jet energy scale has been varied, and the $\not{E}_T$ recalculated. The resulting uncertainty is below 1%.

Since we do not observe any significant excess in the data, an upper limit is set on the production cross section times branching fraction $\sigma_{W'} \times B(W' \to e\nu)$. The limit is derived using a binned likelihood for the whole transverse mass spectrum with 140 GeV $< m_T < 1000$ GeV. The individual shape-changing systematic uncertainties (up and down variation) enter the limit calculation via individual histograms; bin correlations are taken into account. A Bayesian approach [21] is used to calculate upper limits on the cross section for different resonance

TABLE I: Event numbers in the data compared to the background prediction after applying the cut on the transverse mass $m_T > 140$ GeV. For the signal and background processes statistical and systematic uncertainties are given.

Process	Events	stat	sys
Data	**967**		
Sum of backgrounds	959	21	90
$W \to e\nu$	875	20	90
QCD multijet (from data)	27	2	2
other	57	3	4
$W' \to e\nu$			
$m_{W'} = 500$ GeV	1169	24	86
$m_{W'} = 600$ GeV	393	8	32
$m_{W'} = 700$ GeV	147	3	13
$m_{W'} = 800$ GeV	51	1.1	5.4
$m_{W'} = 900$ GeV	19	0.4	2.4
$m_{W'} = 1000$ GeV	7.4	0.2	1.1
$m_{W'} = 1100$ GeV	3.4	0.1	0.5
$m_{W'} = 1200$ GeV	1.7	0.1	0.2

masses. A Poisson distribution is assumed for the number of expected events in each bin of the transverse mass distribution, as well as flat prior probabilities for the signal cross sections. The prior for the combined signal acceptance and background yields is a multivariate Gaussian with uncertainties and correlations described by the corresponding covariance matrix. The observed and expected 95% C.L. limits on the production cross section times branching fraction $\sigma_{W'} \times B(W' \to e\nu)$ are shown in Fig. 3. The lower bound of the theoretical cross section is used to obtain the mass limit. Hence, an additional heavy charged gauge boson with mass below 1.00 TeV is excluded at the 95% C.L.

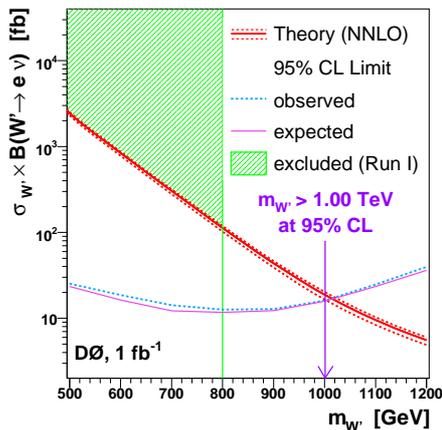In summary, a search for a new heavy charged gauge boson W' decaying to an electron and a neutrino has

FIG. 3: The observed and expected 95% C.L. limits on the cross section as a function of the mass of the W' boson, including statistical and systematic uncertainties. The expected limit assumes a background-only hypothesis. The theoretical expectation is displayed with its uncertainty. Also shown is the D0 Run I limit [5].

been performed using 1 fb^{-1} of data collected with the D0 detector in Run II. We do not observe an excess in the data, and set upper limits on the cross section times branching fraction, which are of the order of 10 – 40 fb for W' boson masses of 500 GeV $< m_{W'} <$ 1200 GeV. Further, a lower limit on the mass of the W' boson is derived, assuming that the new gauge boson as introduced in [2] has the same couplings to fermions as the SM W boson. We exclude a W' boson with $m_{W'} <$ 1.00 TeV at the 95% C.L. This result represents the most stringent limit on the mass of a charged heavy gauge boson beyond the standard model to date.

[a] Visitor from Augustana College, Sioux Falls, SD, USA.
[b] Visitor from The University of Liverpool, Liverpool, UK.
[c] Visitor from ICN-UNAM, Mexico City, Mexico.
[d] Visitor from II. Physikalisches Institut, Georg-August-University Göttingen, Germany.
[e] Visitor from Helsinki Institute of Physics, Helsinki, Finland.
[f] Visitor from Universität Zürich, Zürich, Switzerland.
[†] Fermilab International Fellow.
[‡] Deceased.

[1] R. N. Mohapatra, Unification and Supersymmetry, Springer (2003).
[2] G. Altarelli et al., Z. Phys. C 45, 109 (1989).
[3] J. C. Pati and A. Salam, Phys. Rev. D 10, 275 (1974); R. N. Mohapatra and J. C. Pati, Phys. Rev. D 11, 566 (1975), 11, 2558 (1975); G. Senjanovic and R. N. Mohapatra, Phys. Rev. D 12 1502 (1975).
[4] S. Abachi et al. (D0 Collaboration), Phys. Rev. Lett. 76, 3271 (1996).
[5] V. M. Abazov et al. (D0 Collaboration), Phys. Rev. D 69, 111101 (2004).
[6] V. M. Abazov et al. (D0 Collaboration), Phys. Lett. B 641, 423 (2006).
[7] T. Affolder et al. (CDF Collaboration), Phys. Rev. Lett. 87, 231803 (2001).
[8] D. Acosta et al. (CDF Collaboration), Phys. Rev. Lett. 90, 081802 (2003).
[9] A. Abulencia et al. (CDF Collaboration), Phys. Rev. D 75, 091101 (2007).
[10] V. M. Abazov et al. (D0 Collaboration), Nucl. Instrum. Methods A 565, 463 (2006).
[11] T. Andeen et al., FERMILAB-TM-2365 (2006).
[12] T. Sjöstrand et al., Comput. Phys. Commun. 135, 238 (2001).
[13] J. Pumplin et al., JHEP 0207 012 (2002) and D. Stump et al., JHEP 0310 046 (2003).
[14] R. Brun and F. Carminati, CERN Program Library Long Writeup W5013, 1993 (unpublished).
[15] R. Hamberg, W. L. van Neerven and T. Matsuura, Nucl. Phys. B359, 343 (1991); Erratum-ibid. B644, 403 (2002).
[16] N. Kidonakis and R. Vogt, Phys. Rev. D 68, 114014 (2003).
[17] J. M. Campbell and R. K. Ellis, Phys. Rev. D 60, 113006 (1999).
[18] The azimuth angle ϕ is defined in the plane perpendicular to the beams, with $\phi = \pi/2$ pointing up.
[19] G.C. Blazey et al., in Proceedings of the Workshop: QCD and Weak Boson Physics in Run II, edited by U. Baur, R.K. Ellis, and D. Zeppenfeld, FERMILAB-PUB-00/297 (2000).
[20] W.-M. Yao et al., Journal of Physics G 33, 1 (2006).
[21] I. Bertram et al., FERMILAB-TM-2104 (2000).